

Enhanced Photoacoustic Beam Profiling of Pulsed Lasers

**M. González, G. Santiago, M. Paz,
V. Slezak & A. Peuriot**

**International Journal of
Thermophysics**
Journal of Thermophysical Properties
and Thermophysics and Its Applications

ISSN 0195-928X

Int J Thermophys
DOI 10.1007/s10765-013-1437-8

Volume 34 • Number 2 • February 2013

**ONLINE
FIRST**

International
Journal of
Thermophysics

Available
online
www.springerlink.com

IJOT • 10765 • ISSN 0195-928X
34(2) 191–384 (2013)

 Springer

 Springer

Your article is protected by copyright and all rights are held exclusively by Springer Science +Business Media New York. This e-offprint is for personal use only and shall not be self-archived in electronic repositories. If you wish to self-archive your article, please use the accepted manuscript version for posting on your own website. You may further deposit the accepted manuscript version in any repository, provided it is only made publicly available 12 months after official publication or later and provided acknowledgement is given to the original source of publication and a link is inserted to the published article on Springer's website. The link must be accompanied by the following text: "The final publication is available at link.springer.com".

Enhanced Photoacoustic Beam Profiling of Pulsed Lasers

M. González · G. Santiago · M. Paz ·
V. Slezak · A. Peuriot

Received: 27 January 2012 / Accepted: 4 April 2013
© Springer Science+Business Media New York 2013

Abstract An improved version of a photoacoustic beam profiler of pulsed lasers is presented. The new model resorts to high-bandwidth condenser microphones to register higher-order, excited acoustic modes, thus enabling more accurate profiling. In addition, Xe was used as a buffer gas since its high atomic weight further reduces the eigenfrequencies. Furthermore, a new gas-handling system makes up for some deficiencies found in the first model. The system was calibrated using the Airy pattern generated with a pinhole illuminated by a frequency-doubled Nd:YAG laser that excited NO₂ traces. Once calibrated, the beam profile of a TEA CO₂ laser was obtained, using ethylene as the absorbing species. This profiler returns more accurate profiles than thermal paper.

Keywords Laser beam profiling · Pulsed photoacoustics · Acoustic modes

1 Introduction

In a previous study [1], we reported on the development of a prototype for photoacoustic beam profiling of pulsed lasers. We analyzed how to reconstruct the intensity profile of the laser beam from the recorded acoustic signals, measured by two microphones. The method assumes that the initial pressure distribution inside the acoustic cell follows the intensity pattern if the absorbed energy relaxes rapidly compared to the

M. González · G. Santiago (✉) · M. Paz
Laboratorio Láser, Facultad de Ingeniería, Universidad de Buenos Aires,
Paseo Colón 850, 1063 Buenos Aires, Argentina
e-mail: gsantia@fi.uba.ar

V. Slezak · A. Peuriot
Centro de Investigaciones en Láseres y Aplicaciones CITEDEF,
J. B. Lasalle 4397, 1603 Buenos Aires, Argentina

shortest period of the acoustic signal. This initial pressure condition can be described as a superposition of acoustic modes with different amplitudes and phases.

The general behavior of these modes is that of a damped oscillation at the acoustic cell's eigenfrequencies.

Briefly explained, the algorithm retrieves the initial amplitudes and phases through the Fourier transform of the recorded acoustic signals of two microphones placed at selected positions on the wall of a cylindrical cell.

Initially, we tested the idea by reconstructing the mode of a frequency-doubled Nd:YAG laser.

Even though the first prototype served to show the principle of operation, it had some drawbacks. Because of the low bandwidth of the microphones (≈ 10 kHz), we were able to register a few excited acoustic modes. To make up for this limit, we used Freon 12 as the buffer gas; in this way we reduced the speed of sound to about one-half the value in air and, in the same proportion, the resonant frequencies.

This frequency limitation made it impossible to measure beams below 14/16 mm in diameter. This is a rather high value for many lasers, and it demanded the use of a beam expander, a cumbersome procedure indeed.

The gas-handling pipes caused another problem that showed up as a distortion of the acoustic modes of the cylindrical cell. In a geometrically perfect one, the transverse modes are described by Bessel functions multiplied by sine/cosine terms. However, the former Pyrex cell was not perfectly round and the glass pipe that served for gas-handling purposes had a rather large diameter (~ 5 mm) and length (~ 20 mm). These defects affected the mode pattern.

A numerical simulation of our cell revealed that those imperfections distorted the "radial" modes into an elliptical pattern. Since the recovering algorithm uses the Bessel functions, some amount of mismatching between the actual and the reconstructed beam was always present.

In this paper we introduce a new, improved model, with hardware and software enhancements. The new system made it possible to measure more accurately the fluence of a TEA CO₂ laser that was the light source in another photoacoustic experiment [2].

2 Experimental Apparatus and Results

We started by extending the acoustic bandwidth and replaced the hearing-aid microphones we had used (Knowles EK-3132, FET amplifier) with studio recording Aco Pacific 7017 model (bandwidth ≈ 70 kHz, average sensitivity -50 dB (1 V/Pa), 6.35 mm diameter) condenser microphones. The extended bandwidth comes at the expense of a lower sensitivity (≈ 10 dB @ 1 kHz) and the necessity of a 200 V, low-noise bias supply because these microphones are not of the electret type. Furthermore, the new microphones lack the standard amplifier found in hearing-aid models. Since standard studio preamplifiers are too bulky to suit our mechanical requirements, we designed and built a new, low noise, current-to-voltage preamplifier whose discrete FET front stage shows very low input current noise, an important issue resulting from the high output impedance of the microphone. To take advantage of the microphone's

bandwidth, we had to settle at a transimpedance below 1 k Ω , making it necessary to use a low-noise voltage amplifier (Tektronix AM 502). As a digitizer, we used a National Instruments 6133 acquisition card (2 MS/s), triggered synchronously with the laser.

In the second place we replaced the old cell with a new one, machined from a solid block of Teflon (36 mm inner diameter, 100 mm long). The gas entered the cell through a smaller orifice (1 mm diameter), and the volume of the incoming pipe was smaller than the original one. These changes served to lessen the influence of the gas-handling system and noticeably reduced the distortion of the acoustic modes, thus expanding the beam reconstructing capabilities of the system. The cell was enclosed by two BK7 windows for operation in the visible region, and ZnSe ones for the IR regions.

In addition, we decided to resort to Xe as the buffer gas. Formerly, we had used Freon 12 because we had restricted ourselves to measurements at 532 nm, a wavelength where Freon 12 shows no absorption. However, we were now interested in IR lasers and Xe is a better choice since it is transparent across the visible and IR regions. The speed of sound in Freon 12 amounts to 48 % of its value in air. With Xe we obtain 50 %, a similar result but without absorption in the IR. A heavier buffer gas determines a lower speed of sound and lower eigenfrequencies that fit within the acoustic bandwidth. Figure 1 shows the spectra of two photoacoustic signals, one acquired with N₂ and the other with Xe; the difference is quite noticeable.

Since the speed of sound changes with temperature (and thus the eigenfrequencies), we decided to add an automated register of temperature through a simple LM35 temperature sensor and one of the spare inputs of the acquisition card. This enabled in-time scaling of the eigenfrequencies.

Finally, we made a change to the algorithm. A perfect photoacoustic signal shows a spectrum whose amplitude, between resonances, is negligible. However, in the real

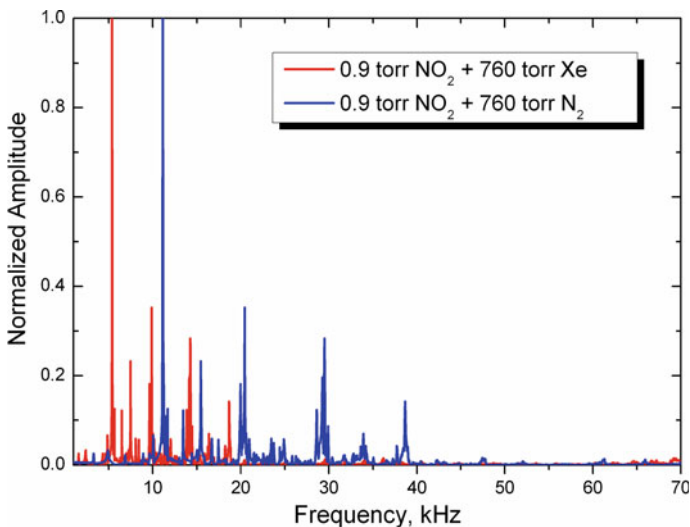


Fig. 1 Influence of buffer gas atomic weight on resonance frequencies

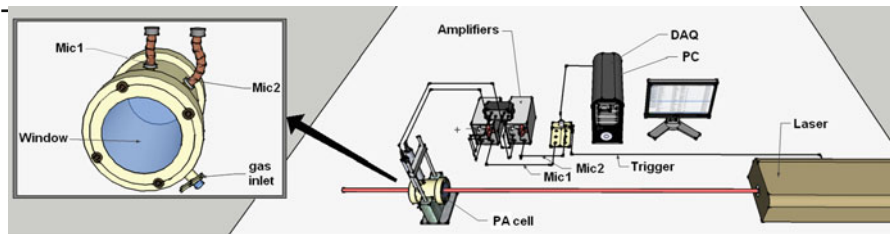


Fig. 2 Experimental setup

world, the system picks up noise and this demands applying some threshold. In effect, the part of the algorithm that finds the amplitude in the vicinity of a resonance must discard the record if it is too close to the rms value of noise. Otherwise, the recovered beam would show fictitious results. In the original prototype we simply resorted to operator expertise. Now, we included a variable threshold, computed from the standard deviation of the registered signal far from the allowed resonances. If the signal spectrum amplitude, close to one of the eigenfrequencies, approaches the threshold value, the algorithm discards that mode. This bandwidth-limiting procedure leads to a system less capable of resolving small details, but the benefits in noise-reduction outweigh the drawback. We specially used this feature in noisy environments (electrically pulsed lasers). The algorithm also returns the reconstructed beam without bandwidth-limiting, but this feature is seldom useful. Reducing the threshold, particularly by better shielding, is under development.

We calibrated the apparatus by recovering the Airy pattern produced with a pinhole illuminated by a frequency-doubled Nd:YAG laser that excites NO_2 (0.9 Torr) diluted in Xe up to 760 Torr (Fig. 2). At this pressure the deactivation time of excited NO_2 is, at most, 10 ns [3], a time that fulfills the main assumption about the relaxation. A uniformly illuminated disk of diameter d produces an Airy pattern whose first null, at distance L , has a diameter $D \approx \frac{2.44 \lambda L}{d}$ (λ : laser wavelength). We used pinholes of diameter $d = 0.4$ mm, 0.7 mm, and 1 mm, and the profiler was placed 2.25 m behind the pinholes. Even though each microphone's frequency response was available from the manufacturer, we had to take into account minor differences between them (not seen in logarithmic scale) as well as lack of perfect matching of the preamplifiers. We adjusted the system's amplitude and phase response until the reconstructed Airy pattern was closest to the theoretical one.

The results can be seen in Figs. 3, 4, 5, and 6. In the first three we have superimposed a few black rings that signal the position of the first nulls of the Airy disk. However, we carefully tried to align the cell's axis to the light beam, we could not avoid some mismatching and some azimuthal modes were excited. Clearly, a perfect system should be able to deal with this situation but our system cannot register azimuthal modes of order higher than four. This is the reason the reconstructed patterns do not show perfect symmetry. In spite of this problem, it can be seen that the apparatus is now capable of resolving closely spaced rings. The sixth figure shows the reconstructed laser beam without pinholes.

Having calibrated the profiler, we measured the far field beam of a dot-mirror TEA CO_2 laser [4], by exciting ethylene (30 Torr) in Xe (up to 760 Torr again). Ethylene has

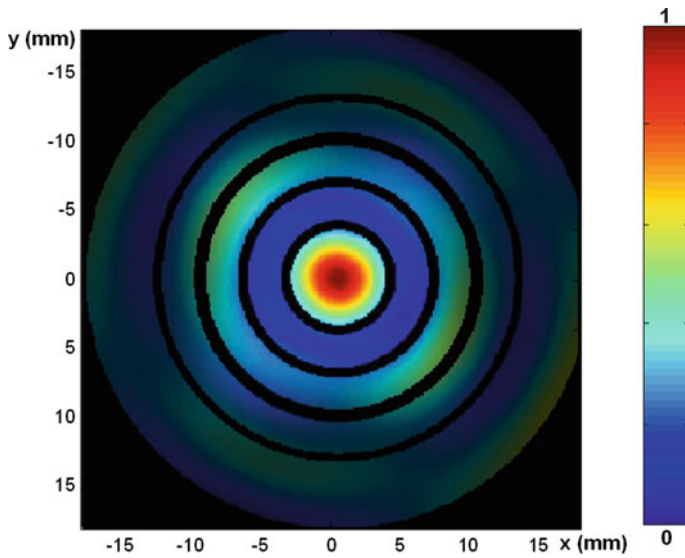


Fig. 3 Reconstructed Airy pattern: iris diameter 0.4 mm, distance to profiler 2.25 m

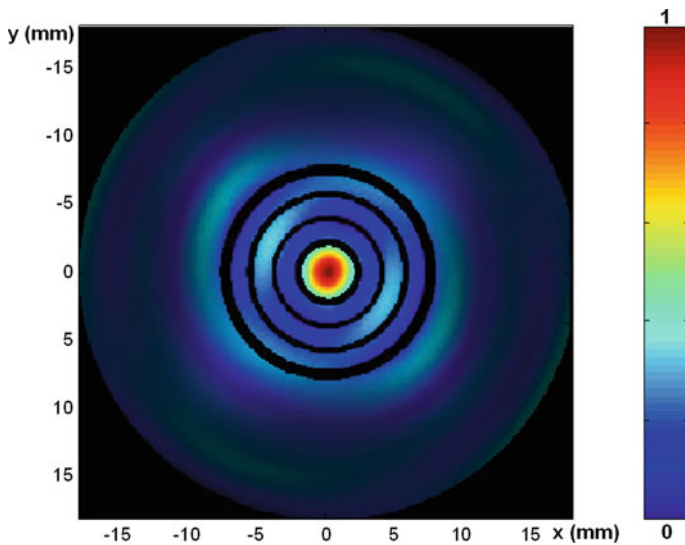


Fig. 4 Reconstructed Airy pattern: iris diameter 0.7 mm, distance to profiler 2.25 m

strong absorption at the 10P(14) line, but that transition also shows strong saturation. Therefore, we decided to tune the laser at the 10P(18) line in order to trade sensitivity for linearity. The deactivation time of ethylene is about $4 \mu\text{s}$ [5], a value noticeably longer than that of NO_2 , but still short enough to satisfy our assumptions. In this case we changed the BK7 windows we had used to calibrate the apparatus for ZnSe ones. Figure 7 presents the reconstructed beam and Fig. 8 depicts a scanned version of the

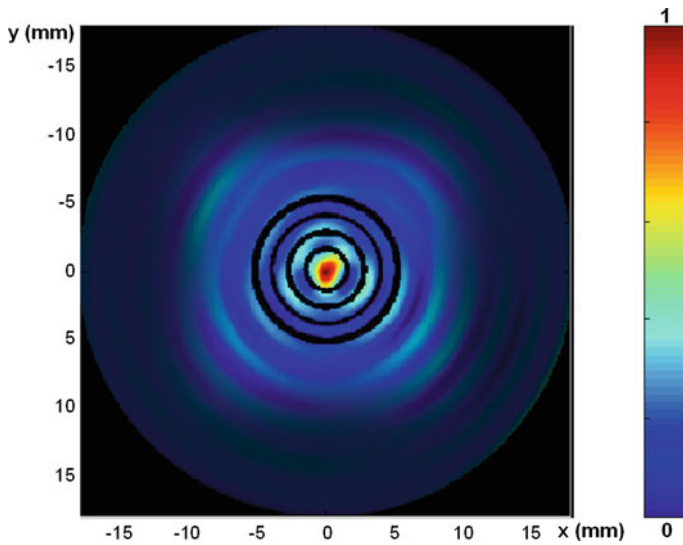


Fig. 5 Reconstructed Airy pattern: iris diameter 1 mm, distance to profiler 2.25 m

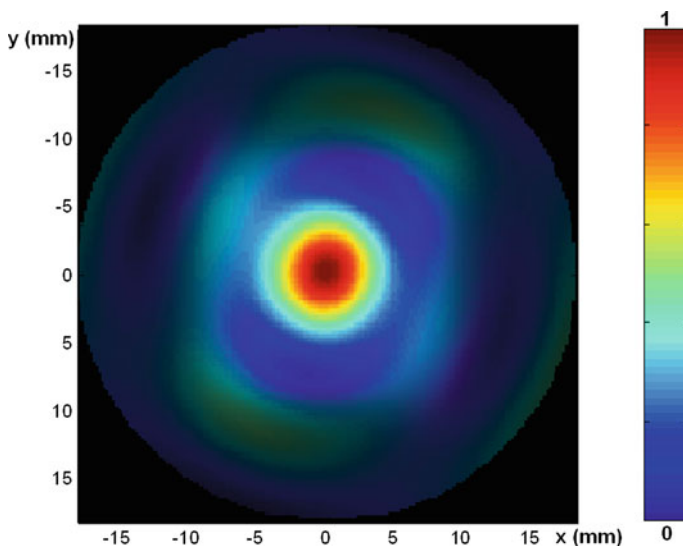


Fig. 6 Reconstructed Nd:YAG laser beam (no diaphragms)

register on thermal paper. Even though both images return about the same size, the photoacoustic profiler reveals the presence of a central peak, absent in the “flattened” image on thermal paper. This laser was used in another photoacoustic experience [2] on ammonia and the photoacoustic profiler helped us compute the fluence more accurately, an important issue when dealing with saturation effects.

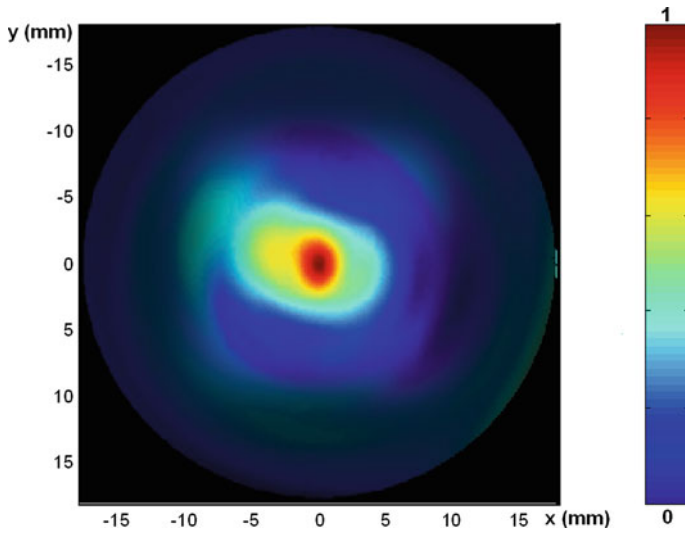


Fig. 7 Reconstructed TEA CO₂ laser beam

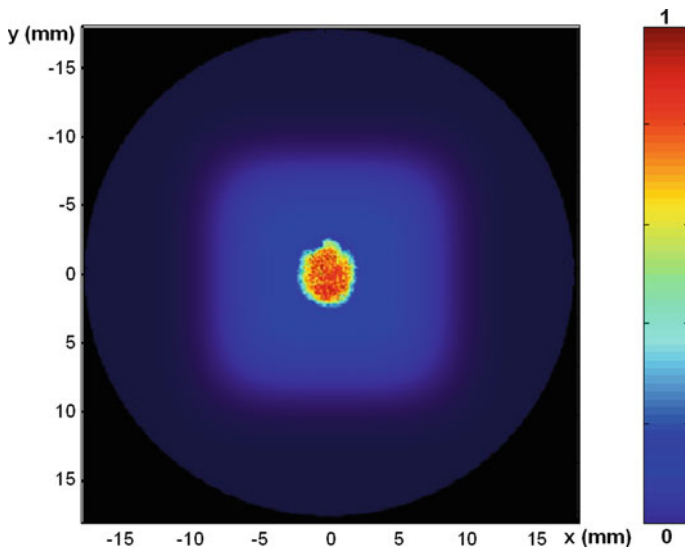


Fig. 8 Record on thermal paper of the TEA laser mode

3 Conclusion

The new version of the photoacoustic beam profiler is capable of measuring features of about 2 mm, a noticeable improvement (approximately sevenfold) over the original one. Most of the improvement stems from the large bandwidth microphones and tighter mechanical tolerances. The automated temperature recording and the bandwidth-limiting in the presence of noise ease the profiling procedure. Even though

the photoacoustic beam profiler can not match the resolution of a camera, it can withstand a laser fluence much larger because the absorbing gas can be easily replaced (if necessary) and the damage threshold of most windows is much larger than that of a detector.

Acknowledgments This work was supported by the University of Buenos Aires through the grant UBACYT 20020090100136. We would like to thank Daniel Sinnewald for his help with the low-noise current-to-voltage-converters and José Luque for his expertise on mechanical matters.

References

1. M. González, G. Santiago, V. Slezak, A. Peuriot, *Rev. Sci. Instrum.* **80**, 113106 (2009)
2. A. Vallespi, V. Slezak, A.P. Peuriot, G. Santiago, *Int. J. Thermophys.* doi:[10.1007/s10765-012-1354-2](https://doi.org/10.1007/s10765-012-1354-2)
3. N. Barreiro, A. Vallespi, A. Peuriot, V. Slezak, G. Santiago, *Appl. Phys. B - Lasers Opt.* **99**, 591 (2010)
4. A. Peuriot, G. Santiago, C. Rosito, *Opt. Eng.* **41**, 1903 (2002)
5. I. Calasso, Dissertation, ETH Zurich, 1998, No. 12925